Direct Sol−Gel Replication without Catalyst in an Aqueous Gel System: From a Lipid Nanotube with a Single Bilayer Wall to a Uniform Silica Hollow Cylinder with an Ultrathin Wall

Q. Ji,[†,§] R. Iwaura,[‡] M. Kogiso,[‡,§] J. H. Jung,[§] K. Yoshida,[‡] and T. Shimizu*[,‡,§]

Graduate School of Pure and Applied Sciences, University of Tsukuba, 1-1-1 Tennodai, Tsukuba, Ibaraki 305-8571, Japan, Nanoarchitectonics Research Center (NARC), National Institute of Advanced Industrial Science and Technology (AIST), Tsukuba Central 5, 1-1-1 Higashi, Tsukuba, Ibaraki 305-8565, Japan, and CREST, Japan Science and Technology Agency (JST), Tsukuba Central 4, 1-1-1 Higashi, Tsukuba, Ibaraki 305-8562, Japan

Received May 14, 2003. Revised Manuscript Received October 31, 2003

A combination of transmission electron microscopy (TEM) and atomic force microscopy (AFM) revealed that a secondary ammonium hydrochloride of a peptidic lipid, in which an L-prolyl-L-prolyl-L-proline fragment is coupled with an L-glutamate derivative carrying two long alkyl chains, self-assembles in water to form nanotube structures consisting of a single bilayer wall. Mixing an aqueous dispersion containing the lipid nanotubes with tetraethoxysilane (TEOS) led to slow gelation due to sol−gel condensation in the absence of solution catalyst. TEM analysis of the aqueous gel phase, coupled with electron energy-loss spectroscopy (EELS), revealed the presence of a high population of hybrid nanotube architectures with a well-defined organic/inorganic interface. Lyophilization and subsequent calcination of the aqueous gels produced silica nanotubes with uniform walls 8-nm thick. The weakly acidic and mildly catalytic lipid headgroup is responsible for the characteristic formation of the silica nanotubes. The minimal amount of positive charges on the surfaces of the lipid nanotube also contributes to this mechanism. Thus, in an aqueous gel system, the morphology of the lipid nanotube consisting of a single bilayer wall was replicated directly into a silica nanotube with an ultrathin wall.

Introduction

Isolated tubular architectures with a nanometer-sized hollow cavity have been receiving steadily growing attention in natural science and materials science fields from the viewpoint of their potential applications and the continuing interest in fundamental phenomena specific to a confined nanospace.[1−6] The well-known nanotube architectures to date include, for example, *biological* microtubules based on the self-assembly of tubulin proteins,[7] *physical* carbon nanotubes that are essentially rolled-up graphene sheets,[1,4] and *chemical* nanotube structures based on either one-dimensional stacking of cyclic compounds[5] or hollow-cylindrical assembly of lipid bilayers.[8−10] In particular, several authors have published numerous works on morphosynthesis of pure silicas,[11−14] among these silicas we can refer to the recent development of a series of hollow cylinders consisting of SiO_2, TiO_2, and VO_2. Since the first report by Nemetschek and Hofman in 1953,[15] Baral and Schoen,[16] Mann et al.,[17−19] Nakamura and Matsui,[20] Adachi et al.,[21−23] and Moreau et al.[24] have documented

* To whom correspondence should be addressed. Telephone: +81-29-861-4544. Fax: +81-29-861-4545. E-mail: tshmz-shimizu@aist.go.jp.
† University of Tsukuba.
‡ Nanoarchitectonics Research Center (NARC), AIST.
§ CREST, JST.

(1) For example, see Iijima, S. *Nature* **1991**, *354*, 56−58.
(2) Fuhrhop, J. H.; Spiroski, D.; Boettcher, C. *J. Am. Chem. Soc.* **1993**, *115*, 1600−1601.
(3) Schnur, J. M.; Ratna, B. R.; Selinger, J. V.; Singh, A.; Jyothi, G.; Easwaran, K. R. K. *Science* **1994**, *264*, 945−947.
(4) For example, see Collins, P. G.; Zettl, A.; Bando, H.; Thess, A.; Smalley, R. E. *Science* **1997**, *278*, 100−103.
(5) For example, see Bong, D. T.; Clark, T. D.; Granja, J. R.; Ghadiri, M. R. *Angew. Chem., Int. Ed.* **2001**, *40*, 988−1011.
(6) Shimizu, T. *Macromol. Rapid Commun.* **2002**, *23*, 311−331.
(7) For example, see Mitchison, T.; Kirshner, M. *Nature* **1984**, *312*, 232−237.
(8) Yager, P.; Schoen, P. E. *Mol. Cryst. Liq. Cryst.* **1984**, *106*, 371−381.
(9) Yamada, K.; Ihara, H.; Ide, T.; Fukumoto, T.; Hirayama, C. *Chem. Lett.* **1984**, 1713−1716.
(10) Nakashima, N.; Asakuma, S.; Kunitake, T. *J. Am. Chem. Soc.* **1985**, *107*, 509−510.
(11) Mann, S.; Ozin, G. A. *Nature* **1996**, *382*, 313−318.
(12) Lin, H.-P.; Mou, C.-Y. *Science* **1996**, *273*, 765−768.
(13) Zhao, D.; Feng, J.; Huo, Q.; Melosh, N.; Fredrickson, G. H.; Chmelka, B. F.; Stucky, G. D. *Science* **1998**, *279*, 548−552.
(14) Ying, J. Y.; Mehnert, C. P.; Wong, M. S. *Angew. Chem., Int. Ed.* **1999**, *38*, 56−77.
(15) Nemetschek, T.; Hofmann, U. *Z. Naturforsch.* **1953**, *8b*, 410−412.
(16) Baral, S.; Schoen, P. *Chem. Mater.* **1993**, *5*, 145−147.
(17) Archibald, D. D.; Mann, S. *Nature* **1993**, *364*, 430−433.
(18) Shenton, W.; Douglas, T.; Young, M.; Stubbs, G.; Mann, S. *Adv. Mater.* **1999**, *11*, 253−256.
(19) Dujardin, E.; Peet, C.; Stubbs, G.; Culver, J. N.; Mann, S. *Nano Lett.* **2003**, *3*, 413−417.
(20) Nakamura, H.; Matsui, Y. *J. Am. Chem. Soc.* **1995**, *117*, 2651−2652.
(21) Adachi, M.; Harada, T.; Harada, M. *Langmuir* **1999**, *15*, 7097−7100.

10.1021/cm034356w CCC: $27.50
Published on Web 12/23/2003

Scheme 1

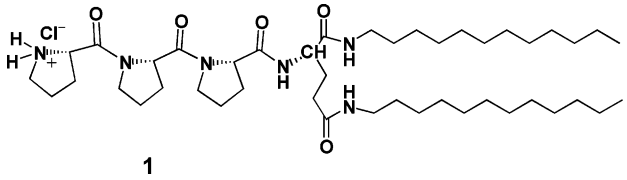

1

stimulating work on silica nanotube fabrication. In addition, Shinkai,[25−31] Hanabusa,[32,33] and their coworkers have done extensive work on an intriguing methodology of sol−gel reaction of metal alkoxide using organogels as a template. Thus, surfactant-mediated or organogel-templated fabrication of silica nanotubes has gradually improved their size and shape uniformity as defined by the inner and outer diameters, the wall thickness, and the tube lengths.[27]

However, it should be noted here that neither of the two methods can reproduce an exact copy through current sol−gel processes. Typically, *rod*-shaped molecular assemblies can produce *tubular* morphologies of metal oxide.[34] Similarly, the morphology of a helical fiber, tubule, or double-helical rope could turn out to be helical tubes,[33] double-layered tubes,[35] or double-helical nanotubes,[36] respectively. It is also important for us to clarify the mechanism of the silica fabrication during sol−gel condensation, which varies sensitively depending on the experimental procedures.[22,37] Here we describe the duplication of a certain nanotube structure from organomolecule-based to silica-based materials. In other words, the present procedure can provide a way for close reproduction of a nanotube shape by using molecular assemblies as a template. We employed the synthetic cationic lipid **1** (Scheme), which can self-assemble into nanotube structures, in place of common surfactants.[21,38] We used only water as a reaction solvent,[39] which contained no active solution catalysts such as H^+, OH^-, or benzylamine.[37,39] Therefore, the present methodology clearly differs from the so-called surfactant-mediated system in aqueous media[21] and from the organogel-templated system in organic solvent.[25,27] A relatively low population of positive charges and a very mildly catalytic site on the organic templates are crucial for the formation of the characteristic nanotube having a smooth and ultrathin silica wall.

Experimental Section

Materials and General Methods. The peptidic lipid **1**[40,41] consisting of tri-proline and glutamic acid dialkyl amide was synthesized in a way similar to the method described previously.[42] The molecular structure was determined by ^{1}H NMR, FT-IR, elemental analysis, and mass spectrometry. ^{1}H NMR spectra were recorded on a JEOL 600 spectrometer. For the FT-IR measurement, a Jasco FT-IR-620 (resolution 4 cm^{-1}) was used. FAB-MS spectra were measured using a JEOL DX303. XRD was measured with a Rigaku diffractometer (Type 4037) using graded *d*-space elliptical side-by-side multilayer optics, monochromated Cu Kα radiation (40 kV, 30 mA), and an imaging plate (R-Axis IV). For the atomic force microscopy (AFM) measurements, a droplet of an aqueous dispersion containing nanotubes [lipid **1** = 0.1% (w/v)] was placed on a clean mica substrate and dried overnight at atmospheric pressure in an electric desiccator. The morphology and the cross-section profile were observed using a commercial atomic force microscope (Digital Instruments, Inc., Nanoscope IIIa).

TEM and SEM Measurement. For energy-filtering transmission electron microscopy (EF-TEM), a droplet of the same aqueous dispersion as used for the AFM measurement was placed on a carbon-coated copper grid (400 mesh). The grid was then dried under vacuum for 1 h. Unstained specimens were examined with a Zeiss LEO 912 Omega, at an accelerating voltage of 120 kV. Scanning TEM (STEM) was also done in a field emission scanning electron microscope (FE-SEM) (Hitachi S-4800) in TEM mode at an accelerating voltage of 15 kV. For the STEM, negatively stained samples were prepared with 2% (w/v) phosphotungstic acid. The pH was adjusted to 7.5 with sodium hydroxide. A small amount of the staining solution was applied to the copper grid and allowed to dry at room temperature for 2 min. The staining solution was then blotted off with filter paper, and the samples were dried in a desiccator at room temperature for 2 days. FE-SEM images were taken on a Hitachi S-4800. Electron energy-loss spectroscopy (EELS) was also carried out with a Zeiss LEO 912 Omega, using an accelerating voltage of 120 kV on carbon microgrids. Elemental maps were obtained by subtracting the background intensities under core-loss edges using the three-window technique.

Sol−Gel Process. Lipid **1** (5 mg) was dispersed in deionized water (1 mL) at 50 °C for 5 min by ultrasonication (Branson ultrasonicator model 1200, 47 Hz, 60 W). The obtained aqueous dispersion was then allowed to gradually cool to room temperature and to stand overnight at room temperature. To this aqueous dispersion (0.1 mL) was added tetraethoxysilane (TEOS, 5 mg) at room temperature. The fluid reaction mixture was allowed to stand for 7 days, resulting in gelation. The obtained aqueous gels were freeze-dried under vacuum (1 Pa) at −80 °C for 24−48 h (freeze-dryer Eyela FDU-1200).

Results and Discussion

Gelation of Aqueous Dispersion. Lipid **1** was dispersed in deionized water at 50 °C, which corresponds to a temperature above the phase transition

(22) Adachi, M.; Harada, T.; Harada, M. *Langmuir* **2000**, *16*, 2376−2384.
(23) Harada, M.; Adachi, M. *Adv. Mater.* **2000**, *12*, 839−841.
(24) Moreau, J. J. E.; Vellutini, L.; Man, M. W. C.; Bied, C.; Bantignies, J.-L.; Dieudonne, P.; Sauvajol, J.-L. *J. Am. Chem. Soc.* **2001**, *123*, 7957−7958.
(25) Ono, Y.; Nakashima, K.; Sano, M.; Kanekiyo, Y.; Inoue, K.; Hojo, J.; Shinkai, S. *Chem. Commun.* **1998**, 1477−1478.
(26) Ono, Y.; Nakashima, K.; Sano, M.; Hojo, J.; Shinkai, S. *J. Mater. Chem.* **2001**, *11*, 2412−2419.
(27) von Bommel, K. J. C.; Friggeri, A.; Shinkai, S. *Angew. Chem., Int. Ed.* **2003**, *42*, 980−999.
(28) Jung, J. H.; Ono, Y.; Shinkai, S. *Langmuir* **2000**, *16*, 1643−1649.
(29) Jung, J. H.; Ono, Y.; Shinkai, S. *Angew. Chem., Int. Ed.* **2000**, *39*, 1862−1865.
(30) Jung, J. H.; Ono, Y.; Hanbusa, K.; Shinkai, S. *J. Am. Chem. Soc.* **2000**, *122*, 5008−5009.
(31) Jung, J. H.; Ono, Y.; Sakurai, K.; Sano, M.; Shinkai, S. *J. Am. Chem. Soc.* **2000**, *122*, 8648−8653.
(32) Kobayashi, S.; Hanabusa, K.; Hamasaki, N.; Kimura, M.; Shirai, H. *Chem. Mater.* **2000**, *12*, 1523−1525.
(33) Kobayashi, S.; Hamasaki, N.; Suzuki, M.; Kimura, M.; Shirai, H.; Hanabusa, K. *J. Am. Chem Soc.* **2002**, *124*, 6550−6551.
(34) Jung, J. H.; Shinkai, S.; Shimizu, T. *Nano Lett.* **2002**, *2*, 17−20.
(35) Jung, J. H.; Kobayashi, H.; Masuda, M.; Shimizu, T.; Shinkai, S. *J. Am. Chem Soc.* **2001**, *123*, 8785−8789.
(36) Jung, J. H.; Yoshida, K.; Shimizu, T. *Langmuir* **2002**, *18*, 8724−8727.
(37) von Bommel, K. J. C.; Shinkai, S. *Langmuir* **2002**, *18*, 4544−4548.
(38) Singh, P. S.; Kosuge, K. *Chem. Lett.* **1998**, 101−102.
(39) Jung, J. H.; Shimizu, T. *Chem. Lett.* **2002**, 1246−1247.
(40) Shimizu, T.; Mori, M.; Minamikawa, H.; Mato, M. *Chem. Lett.* **1989**, *8*, 1341−1344.
(41) Shimizu, T.; Hato, M. *Thin Solid Films* **1989**, *180*, 179−183.
(42) Shimizu, T.; Hato, M. *Biochim. Biophys. Acta* **1993**, *1147*, 50−58.

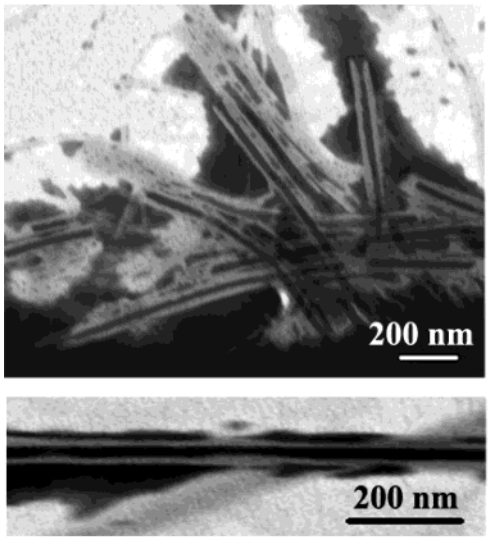

Figure 1. STEM images of the self-assembled tubular structures formed from the peptidic lipid **1** negatively stained with phosphotungstate.

temperature (T_{gl} = 32 °C) of the hydrated sample **1**.[42] We then observed the self-assembled morphologies of lipid **1** using high-resolution TEM. EF-TEM images of the unstained sample gave ribbonlike structures (minor product) and tubular structures (major product) approximately 200-nm wide, although we could detect them only at low black−white contrast (not shown). STEM of the stained samples enabled us to observe clearly the presence of hollow-cylinder structures. Figure 1 displays nanotube structures that encapsulated the stain inside the tube. This finding is compatible with the previous results,[42] proving the formation of well-defined tubular structures through molecular self-assembly. However, in the present work, we were not able to optimize the measurement conditions to evaluate the wall thickness accurately by high-resolution TEM analyses. X-ray diffraction (XRD) measurement of the collected nanotubes displayed no remarkable reflection peaks in the small-angle region, suggesting very thin wall thickness for the nanotube membrane.

To characterize the thickness of the membrane wall, we observed the lipid nanotube formed from **1** in air using AFM.[43] Figure 2 shows an AFM image (2 μm × 2 μm) of the self-assembled nanotube dried in air and its cross-section profile. The height of the nanotube was approximately 8.9 nm on average, corresponding to twice the wall thickness. This finding means that the wall thickness of the nanotube is 4.5 nm. The calculated length of the extended molecule **1** was 2.8 nm by CPK molecular modeling. Thus, all the structural analyses allow us to conclude that the membrane wall of the self-assembled lipid nanotube consists of a single bilayer (Figure 2, lower), in which the lipid molecules are tilted approximately 37° with respect to the plane normal to the layer.

A sol−gel reaction with TEOS is unlikely to occur in the aqueous dispersion in the absence of active solution catalysts such as H^+, OH^-, or benzylamine. However, the aqueous dispersion proved to slowly solidify over a

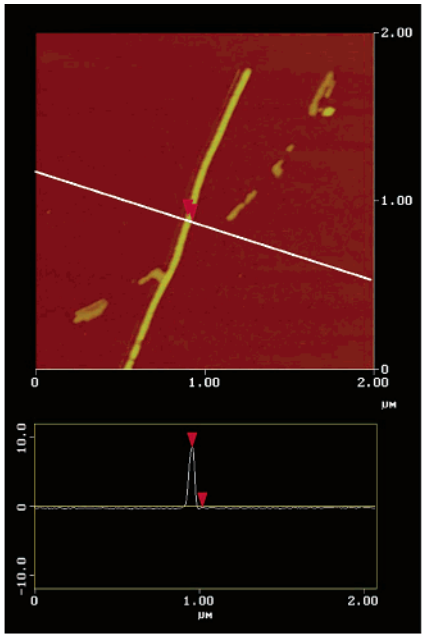

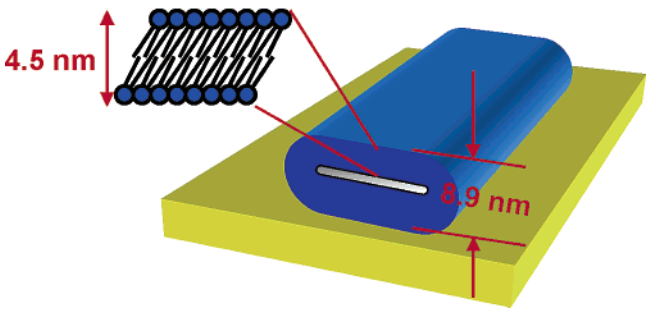

Figure 2. (upper) AFM image (2 μm × 2 μm) of a self-assembled lipid nanotube of **1** and its cross-section profile showing a height of 8.9 nm. (lower) Schematic illustration of the cross section. The flat shape of the nanotube indicates the absence of an aqueous compartment.

period of 7−10 days, eventually resulting in a gel phase. Very interestingly, a TEM image clearly indicated that the solidified gel is composed of abundant nanotube assemblies with uniform size dimensions, i.e., 20-nm wall thickness, 200-nm inner diameters, and 5−10-μm tube length (Figure 3a). To get further insight into the silica distribution in the wall of the organic/inorganic hybrid nanotubes, we also performed elemental mapping of silicon (Si) and carbon (C) by means of EELS analysis coupled with TEM measurements. Figure 3a displays a zero-loss image (EF-TEM image), meaning that incident electrons were scattered by atoms in an elastic fashion. The Si map is shown in Figure 3b, showing the inelastic loss energy of incident electrons caused by the interaction with Si atoms surrounding the organic template. For comparison, the C map is shown in Figure 3c. In Figure 3b, we clearly see two bright lines characteristic of Si mapping at the edge of the hybridized nanotubes. This finding strongly supports the view that the gel formation is induced by templating the organic assemblies and that the silica has thereby been deposited on the surfaces of the organic nanotubes.

Calcination of Xerogels. Unlike well-known one-dimensional nanostructures consisting of organic/inor-

(43) Shimizu, T.; Ohnishi, S.; Kogiso, M. *Angew. Chem., Int. Ed.* **1998**, *32*, 3260−3262.

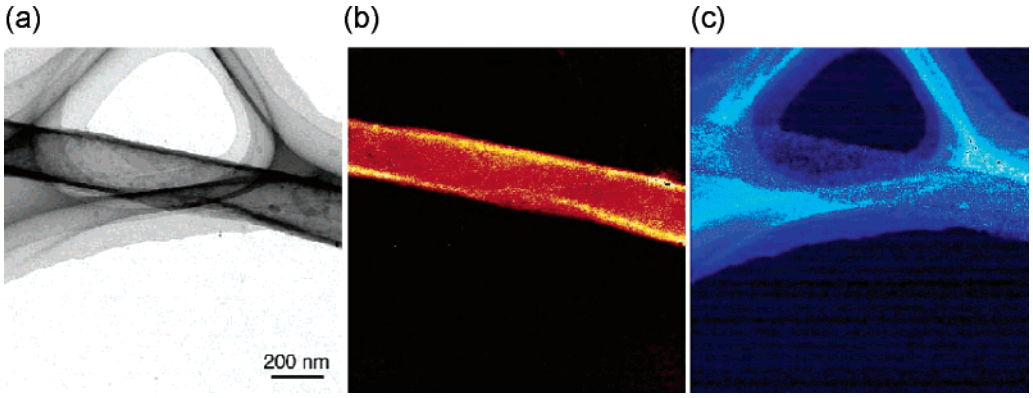

Figure 3. TEM images with electron energy-loss spectroscopy (EELS) of an organic/inorganic hybrid nanotube. (a) Zero-loss image, (b) silicon component, and (c) carbon component before calcination.

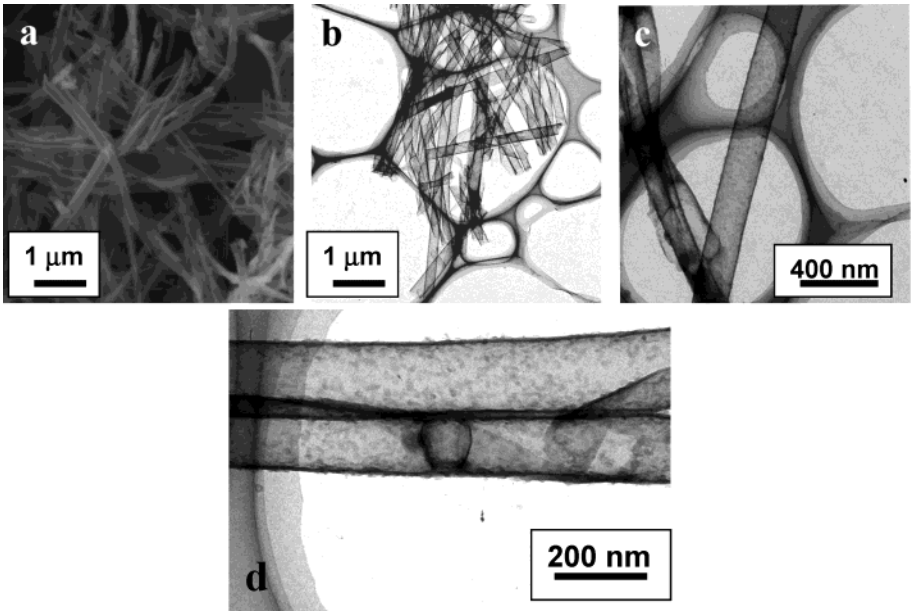

Figure 4. (a) SEM and (b,c) TEM images of uniform silica nanotubes with ultrathin walls after calcination. (d) TEM image of a silica sphere encapsulated in a silica nanotube.

ganic hybrids,[16,20,25,37] the present lipid bilayer membrane and the adsorbed silica layer were ultrathin (thickness 4.5−8 nm). Accordingly, removal of the organic template by calcination resulted in drastic aggregation of silica structures or collapsed nanostructures. Therefore, we lyophilized the aqueous gel under vacuum (1 Pa) for 24−48 h before calcination. The dried material was very light, just like a white sponge. Subsequent calcination of these freeze-dried xerogels gave tubular silica morphologies with uniform shape and size dimensions. Figure 4a shows an SEM image indicating the presence of open-ended silica nanotubes with ultrathin walls, as well as hollow cylinders. A TEM image also proved the wall thickness to be approximately 8 nm. The ratio of the wall thickness to the diameter of the hollow cylinder was approximately 1:25 (Figure 4b and c).

As can be seen in the TEM images (Figure 4b and c), the presence of a silica double layer is not obvious, although it should have appeared after sol−gel polymerization using a tubular structure as an organic template. Though during the TEM measurement we did observe a clear image of a double layer for the silica nanotubes, the nanometer-sized spaces disappeared in a few minutes, probably due to the ultrathin volume, under the present experimental conditions. The 4.5-nm wall thickness of the organic tubular template seems to be too thin to maintain the templated interlayer nanospace. To the best of our knowledge, the present finding may be the first example of silica nanotube fabrication based on templating an organic nanotube with a wall thickness corresponding to a single bilayer. Calcination, which is associated with heat treatment, would generally cause shrinkage of the silica structure, leading to a much greater decrease in nanospace thickness. Both the thinness of the template and the shrinkage of the resultant nanospace are thus responsible for the apparent absence of the interlayer void between the two silica layers.

Another strong piece of evidence for silica adsorption onto the inner surfaces of the tubular template is presented in Figure 4d, which displays a TEM image of a silica nanotube possessing a hollow spherical structure after calcination. On the basis of EELS, this vesicle-like structure was found to be composed of Si, proving it to be a transcribed product from the template. Just like a vesicle-encapsulated microtube from a glycylglycine bolaamphiphile,[44] lipid **1** has also produced vesicles encapsulated within the tubes. Although calcination may have caused some shrinkage and damage

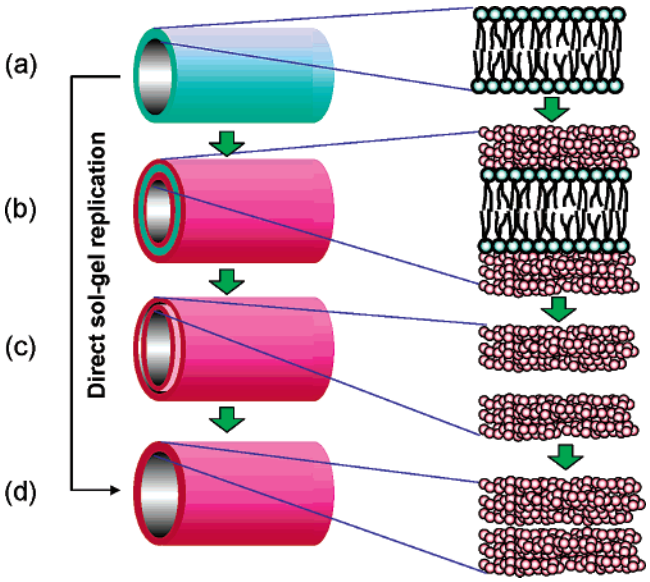

Figure 5. Possible mechanism for the direct sol−gel replication in an aqueous gel system. (a) A lipid nanotube with a single bilayer wall is formed from **1**, (b) a minimum amount of silica precursor is deposited onto the template surfaces due to electrostatic interaction, (c) a silica nanotube with a void the same size as the void in the organic template remains just after calcination, and (d) the silica nanotube is aged to shrink the interlayer void. Thus, a nanotube architecture with wall thickness similar to that of the lipid nanotube can be exactly reproduced with pure silica.

of the replicated Si structure, several Si vesicles have remained intact within the nanotubes. This finding clearly supports that adsorption of silica precursors also takes place on the inner surfaces of the tubes.

Sol−Gel Reaction Mechanism. Generally, acid or base solution catalysts play an indispensable role in initiating and accelerating the hydrolysis of silica precursors and the subsequent sol−gel condensation.[45] In the present experiment, we added no definitive solution catalysts to the aqueous medium. A similar procedure has already been developed by Adachi et al.,[21,22] who employed common surfactants with a long alkyl chain, like laurylamine, as a nucleation seed rather than a template. It should be noted that the present synthetic lipid **1** can self-assemble in water to form a well-defined tubular structure that acts as a nanotemplate. Furthermore, lipid **1** can not only distribute positive charges all over the surfaces of the resultant organic nanotubes, but it can also function as a very mild acid catalyst in weakly acidic pH conditions (pH = ∼4.8). These two conditions are very crucial and very favorable for the minimal deposition of negatively charged silica precursors. Figure 5 schematically illustrates our proposed mechanism for replicating the shape of lipid nanotubes into silica structures. A sol−gel reaction proceeds in aqueous medium according to "a surface-mediated mechanism"[37] on the outer and inner sides of the single bilayers. The minimal amount of positive charges, due to the thin organic wall, depresses the random accumulation of negatively charged silica oligomers. We also found that the addition of a small amount of OH^- as a base catalyst (pH = 9.6) promoted the sol−gel reaction to yield well-defined nanotubes of 30-nm wall thickness. This finding will be strong evidence for this interpretation.

Conclusion

The shape of lipid nanotubes consisting of a single bilayer membrane was successfully replicated into silica nanotubes having an ultrathin wall 8 nm thick by a direct sol−gel transcription method without solution catalysts in an aqueous gel system. The minimal amount of positive charges of the peptidic lipid on the template not only serves as an adsorbing surface but also has a mildly catalytic function. The newly developed method will certainly contribute to more precise control of metal oxide nanostructures at the nanometer level.

CM034356W

(44) Shimizu, T.; Kogiso, M.; Masuda, M. *Nature* **1996**, *383*, 487−488.
(45) Brinker, C. J.; Svherer, G. W. *Sol−Gel Science*; Academic Press: San Diego, CA, 1990.